ACS OMEGA

http://pubs.acs.org/journal/acsodf

Article

Analysis of Primary Reactions in Biomass Oxidation with O_2 in Hot-Compressed Alkaline Water

Jing-Xian Wang, Jun-ichiro Hayashi,* Shusaku Asano, and Shinji Kudo

Cite This: *ACS Omega* 2021, 6, 4236−4246

Read Online

ACCESS | Metrics & More | Article Recommendations | Supporting Information

ABSTRACT: The present study investigated oxidation of pulverized Japanese cedar with O_2 in hot-compressed alkaline water, employing a newly developed flow-through fixed-bed reactor (percolator). It allowed us to determine the rate of the primary extraction that was free from the secondary reactions of extract in the aqueous phase and those over the residual solid, solubility of extractable matter, and mass transport processes. Quantitative kinetic analysis revealed that the cedar consisted of three kinetic components (C1−C3) that underwent extraction in parallel following first-order kinetics with different rate constants. Further analysis revealed the chemical compositions of the kinetic components, which were mixtures of carbohydrates and lignin. C1 was converted most rapidly by nonoxidative reactions such as alkali-catalyzed hydrolysis, while C2 was converted by oxidative degradation. The product distributions from C1 and C2 (CO_2, lower organic acids, oligosaccharides, acid-soluble, and acid-insoluble lignins) were steady throughout their conversion. Both C1 and C2 thus behaved as single reactants; nevertheless, those were lignin/carbohydrates mixtures. It was also demonstrated that the extraction rate of C2 was proportional to the concentration of dissolved O_2. C3 was the most refractory component, consisting mainly of glucan and very minimally of the lignin, xylan, mannan, galactan, and arabinan.

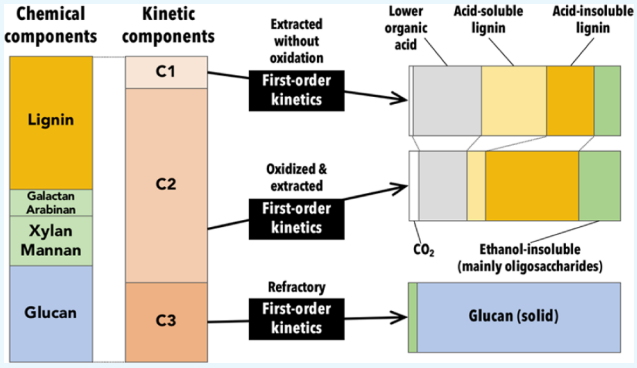

1. INTRODUCTION

Lignocellulosic biomass is the most available and sustainable feedstock, a substantial part of which can be saccharified and transformed to biofuels and chemicals, but not readily digested because of the presence of lignin.[1−4] As a cost-effective and green oxidant, O_2, has widely been used for delignification. The electron transfer between molecular O_2 and lignin can derive active species (radicals) that attack lignin molecules, and break interaromatic unit linkages and also aromatic rings, thereby increasing the solubility.[5] The oxidation of biomass with O_2 in alkaline water is promising for the delignification before production of monosaccharides or bioethanol, if the delignification is selective.[6,7] The oxidation with O_2 removed 30−70% of the lignin and also 10−80% of hemicellulose at 160−200 °C under 0.6−1.4 MPa O_2, improving the accessibility of the solid to enzyme and other properties relevant to enzymatic saccharization.[8−10] In those previous studies, however, little attention was paid to the kinetics and mechanism of the oxidation and delignification.

It is believed that the oxidation involves primary and secondary reactions. The primary reaction is represented by intrasolid degradation. Its rate is equivalent to that of extraction unless it is limited by the solubility of the extractable matter formed. The secondary reactions consist of a homogeneous reaction of the extracted matter in the aqueous (aq) phase and a heterogeneous reaction over the solid being extracted. Understanding of the kinetics and mechanism of the oxidation requires distinguishing those sequential reactions from each other, which can hardly be achieved by adopting conventional batch reactors. Another issue of batch reactors is accumulation of extract with time, in other words, difficulty in defining and maintaining conditions of the aqueous phase.

Kraft pulping has been investigated in detail. It is generally accepted that the pulping process consists of three stages: initial, bulk, and residual stages.[11,12] These are largely influenced by the chemical nature of feedstock, in particular, the reactivity of lignin.[13,14] Most of the previous studies were performed by employing batch reactors with main focus on delignification. Very little information was thus available on the primary and secondary reactions involved in the delignification. The secondary reaction of the lignin- and carbohydrate-derived extracts seemed to occur extensively during delignification.[15−17] Shi et al.[18] recovered a hemicellulose-derived extract from the yellow liquor from a batch Kraft pulping process and

Received: October 22, 2020
Accepted: December 30, 2020
Published: February 4, 2021

https://dx.doi.org/10.1021/acsomega.0c05154
ACS Omega 2021, 6, 4236−4246

found that the recovery was as small as 1.8% of the hemicellulose of the feedstock. This could be due to the secondary degradation of the primary extract. Moreover, the lignin-derived extract could undergo depolymerization or retrogressive condensation in the liquid phase.[19]

Jafari et al.[14,20] studied the kinetics of the delignification in a Kraft pulping applying a continuous flow-through reactor, but they did not focus on the degradation products, the information of which was essential for understanding the mechanism of oxidative degradation and extraction of lignin and carbohydrates. It is known that the oxidative degradation of hemicellulose and that of lignin occur simultaneously.[21] To the best of our knowledge, no systematic information has so far been shown on the primary reaction and extraction in oxidative degradation of either woody biomass or herbaceous and other types of biomass.

The authors of this study designed and employed a flow-through fixed-bed reactor, *i.e.*, percolator, to study the primary degradation and extraction of lignin and carbohydrates from a Japanese cedar during its treatment with hot and compressed alkaline water dissolving O_2, referencing reactor systems adopted to the hydrothermal degradation of cellulose and the hydrothermal degradation of lignite.[22,23] The percolator allowed us to quench the primary extract and analyze its chemical composition. The continuous supply of O_2-saturated alkaline water to the percolator at a sufficiently high rate successfully made the conditions of the alkaline water steady and eliminated mass transfer effects on the kinetics of extraction.[14,24]

2. RESULTS AND DISCUSSION

2.1. Kinetic Analysis and the Primary Reaction Rate.

In every run of the oxidative extraction, O_2 was fed into the percolator at a steady rate. As expected, the rate of O_2 supply was an important factor for the rate of extraction, and this will be discussed later in detail. Charging a sufficiently small amount of the cedar was necessary to avoid the limitation of the rate of extraction by the rate of O_2 supply. Figure 1 shows changes in $1 - X$ with t for different combinations of the initial mass of cedar (m_0) and flow rate of NaOH aq (v). The extraction rate was maximized and independent of both m_0 and v, when $m_0 \leq 0.2$ g and $v \geq 5.0$ mL min^{-1}. It was thus demonstrated that the percolator allowed us to determine the rate of the primary extraction as a function of t. The secondary reaction of the primary extract over the solid was, if any, unlikely to influence the "net" rate of extraction at $m_0 \leq 0.5$ g and $v \geq 5.0$ mL min^{-1}. The secondary reaction of the primary extract in the aqueous phase will be discussed later.

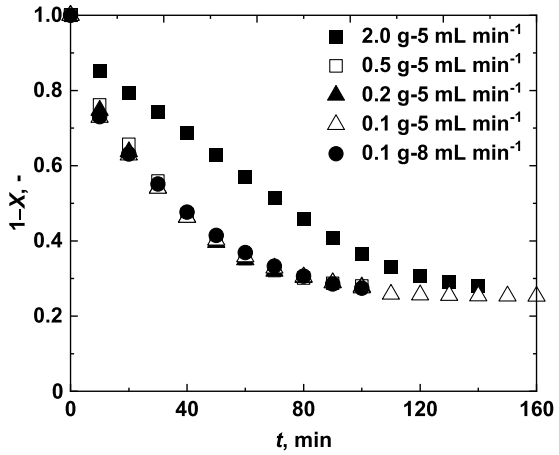

Figure 1. Changes in $(1 - X)$ with t for conditions with different combinations of the initial sample mass (m_0 = 0.1, 0.2, 0.5, or 2.0 g-dry) and flow rate of O_2-saturated 0.1 N NaOH aq (v = 5.0 or 8.0 mL min^{-1}). X is the overall carbon-based conversion.

Figure 2 shows the change in $1 - X$ with t for m_0 = 0.1 g and v = 5.0 mL min^{-1}. $1 - X$ by the primary extraction decreases in an exponential manner to *ca.* 0.25 in 120 min and further decreases afterward but very slowly. This indicates the presence of at least two kinetic components in the cedar. The first emphasis in the kinetic analysis is put on the late-stage extraction. $1 - X$ at $t \geq 150$ min is described well by the following kinetic equation

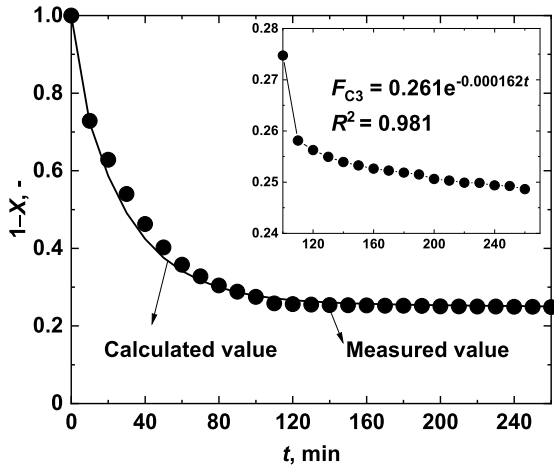

Figure 2. Change in $1 - X$ with t for m_0 = 0.1 g and v = 5.0 mL min^{-1} and extended period of extraction up to t = 260 min.

$$1 - X = 0.26 \exp(-0.000162t) \quad (1)$$

The amount of solid residue after 260 min extraction was insufficient for the analysis of chemical composition, but from a white color of the solid, it seemed that it consisted mainly of cellulose but probably also very smaller fractions of lignin and hemicellulose. This was consistent with previous studies that showed difficulty of complete delignification and also slow delignification on the final stage.[12,25] It is also known that complexes of lignin and cellulose are refractory, being inaccessible to oxygen-containing active species.[26] The chemical composition of the solid residue is shown and discussed quantitatively later.

It was assumed that the cellulose of the cedar consisted of two different parts, *i.e.*, extractable (oxidatively degradable) and refractory parts, and that the latter underwent an extremely slow degradation as expressed by eq 1. The refractory cellulose was, for convenience, termed component-3 (C3). It was also assumed that C3 underwent extraction obeying single first-order kinetics over the range of t.

$$F_{C3} = F_{C3,0} \exp(-k_3 t) = 0.26 \exp(-0.000162t) \quad (2)$$

where $F_{C3,0}$ and F_{C3} are the carbon-based fractions of C3 at t = 0 and t, respectively, and k_3 is the first-order rate constant in a unit of min^{-1}. The value of k_3 is valid only within the range of conditions employed in the present study, *i.e.*, at O_2 concentration in the NaOH aq at 19.6 mmol O_2 L^{-1}.

https://dx.doi.org/10.1021/acsomega.0c05154
ACS Omega 2021, 6, 4236−4246

It was further assumed that the cedar consisted of two kinetic components: C3 and the other (temporarily denoted by C1-2) that underwent extraction simultaneously with C3.

$$F_{C1-2,0} + F_{C3,0} = 1 \quad (t = 0) \tag{3}$$

$$F_{C1-2} + F_{C3} = 1 - X \quad (t = t) \tag{4}$$

F_{C1-2}, defined as the carbon-based fraction of C1-2, was calculated as a function of t from the measured $1 - X$ using eqs 2−4, and is shown in Figure 3. F_{C1-2} seems to decrease with t

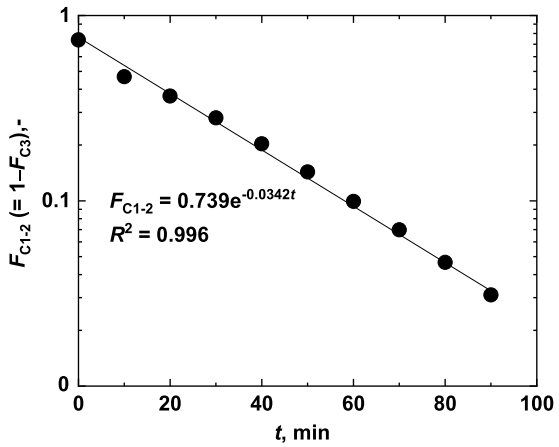

Figure 3. Change in the fraction of C1-2 (F_{C1-2}) with t for m_0 = 0.1 g and v = 5.0 mL min^{-1}.

roughly following first-order kinetics with $F_{C1-2,0}$ = 0.74 (=1 − $F_{C3,0}$) and k_{1-2} = 0.034 min^{-1}. The overall rate of the primary extraction is expressed as

$$1 - X = F_{C1-2,0} \exp(-k_{1-2}t) + F_{C3,0} \exp(-k_3 t) \approx 0.74 \exp(-0.034t) + 0.26 \exp(-0.000162t) \tag{5}$$

Kinetic analysis was performed for some other conditions with combinations of m_0/v = 0.5/5.0, 0.2/5.0, and 0.1/8.0 g/mL min^{-1}, which gave the rate of the primary extraction. The analysis was done with fixed $F_{C1-2,0}$ and $F_{C3,0}$ at 0.74 and 0.26, respectively. The result is shown in Table 1. k_{1-2} falls in a narrow range of 0.034−0.035 min^{-1}, indicating the validity of the kinetic analysis.

Table 1. k_{1-2} Estimated for Different Conditions[a]

m_0/v, g/mL min^{-1}	k_{1-2}, min^{-1}	R^2 for fitting
0.5/5.0	0.0346	0.995
0.2/5.0	0.0350	0.998
0.1/5.0	0.0342	0.996
0.1/8.0	0.0347	0.985

[a] $F_{C1-2,0}$, $F_{C3,0}$, and k_3 were fixed at 0.74, 0.26, and 0.000162 min^{-1}, respectively.

2.2. Further Consideration of Kinetic Components.

Extraction was also carried out under conditions of m_0 = 2.0 g and v = 1.0−7.0 mL min^{-1}, where the rate of extraction was limited by that of O_2 supply due to increased m_0. Those conditions were not applicable to the determination of the primary reaction rate but found to be useful for a deeper understanding of the chemical kinetics and mechanism of the conversion of C1-2. Figure 4 shows the results of kinetic analysis for two conditions as examples. Note that the vertical axes indicate F_{C1-2}, which can be given by $1 - F_{C3}$. F_{C1-2} decreases linearly with t of 60−160 or 10−90 min for v = 1.0 or 5.0 mL min^{-1}, respectively, apparently following zeroth-order kinetics. The pH of the effluent was almost steady around 13 in those periods. Such linearity is attributed to that the rate of extraction was controlled by the steady rate of O_2 supply. In the case of v = 5.0 mL min^{-1} and at t > 90 min, F_{C1-2} decreases exponentially with t. This is reasonable because the residual amount of F_{C1-2} became sufficiently small that the rate of extraction was controlled chemically rather than by the rate of O_2 supply. In fact, as seen in Figure 6, the change in F_{C1-2} at t > 90 min was described well by first-order kinetics with respect to F_{C1-2} with an apparent k_2 of 0.037 min^{-1}. It was very similar to k_{1-2} determined for $m_0 \leq 0.5$ g and $v \geq 5.0$ mL min^{-1}, *i.e.*, 0.034−0.035 min^{-1} (see Table 1).

It is also noted in Figure 4 that the decreases in F_{C1-2} for the initial 60 min (v = 1.0 mL min^{-1}) or 10 min (v = 5.0 mL min^{-1}) are clearly faster than those later. This trend indicates that F_{C1-2} consisted of at least two kinetic components. Then, by assuming the presence of two such components (C1 and C2) in C1-2, the kinetic analysis was done in more detail. The C1 was extracted quickly and completely in the initial 60 min (v = 1.0 mL min^{-1}) or 10 min (v = 5.0 mL min^{-1}). F_{C2} was determined from the linear relationship of F_{C2} *vs* t after complete extraction of C1. The initial fraction of C2 was estimated reasonably by extrapolating the linear relationship between F_{C2} and t to t = 0. As shown in Figure 5, the Y-intercept was almost independent of v over the entire range of v. The average value of the Y-intercepts was 0.635 and then defined as the initial fraction of a subcomponent of F_{C1-2} (C2), *i.e.*, $F_{C2,0}$. The initial fraction of the other subcomponent (C1), $F_{C1,0}$, was automatically given as 0.104 according to $F_{C1-2,0}$ = $F_{C1,0}$ + $F_{C2,0}$.

The extraction of the cedar requires consumption of O_2; therefore, it is necessary to understand the primary reactions and optimize the process. It is, however, very difficult or even impossible to measure the O_2 consumption in a batch reactor due to the secondary oxidative degradation of the extracts. It is worth measuring the O_2 consumption accurately by applying a percolator. Figure 6 plots the apparent rate of C2 extraction that was determined directly from the linear relationship between F_{C1-2} and t, against the rate of O_2 supply. Note that the extraction rate is expressed in mmol C min^{-1}. The rate of extraction is linearly correlated with each other at up to 0.1 mmol min^{-1} O_2 supply. This means that the O_2 dissolved in the NaOH aq was consumed completely or near-completely while passing through the fixed bed and that the O_2 contributed to the degradation and extraction of C2 at an efficiency of 4.7 mol C (mol O_2)$^{-1}$, unless the liquid-phase secondary reaction occurred to a significant degree.

Here, we consider the behavior of C1 that was extracted most rapidly and completely in the early period. It is reasonable to consider that C1 was converted and extracted by particular reactions such as ion exchange (*e.g.*, −COOH + NaOH = −COONa + H_2O) and base-catalyzed hydrolysis of ether/ester bonds, which required no O_2 supply. This idea is consistent with a previous report by Kim et al.[11] who compared the delignification of corn stover under oxidative and nonoxidative conditions and found that a portion of lignin was removed rapidly without oxidation in the initial stage of delignification. In another report, Kataria et al.[27] removed part

https://dx.doi.org/10.1021/acsomega.0c05154
ACS Omega 2021, 6, 4236−4246

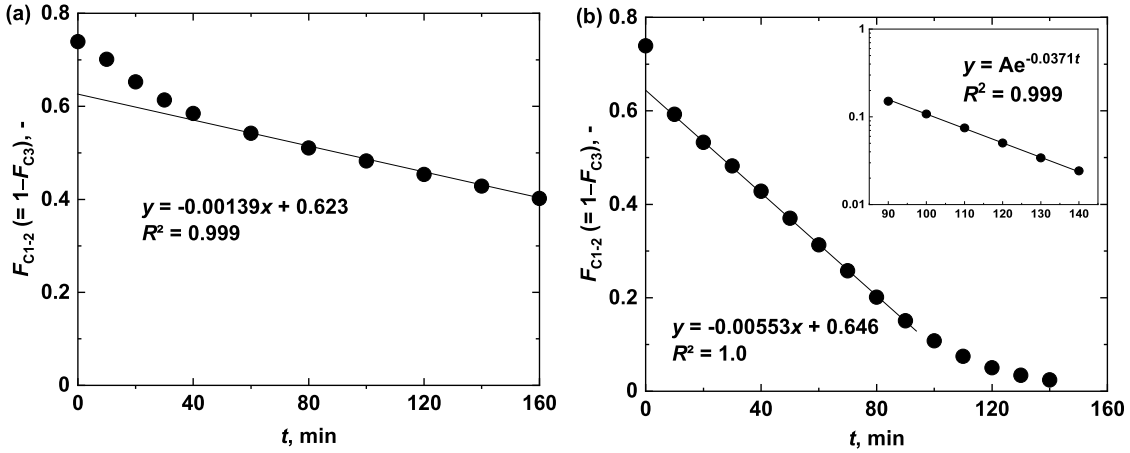

Figure 4. Changes in F_{C1-2} with t for (a) m_0 = 2.0 g and v = 1.0 mL min^{-1} and (b) m_0 = 2.0 g and v = 5.0 mL min^{-1}. $F_{C3,0}$ was calculated by eq 2 with k_3 = 0.26 and 0.000162 min^{-1} for calculating F_{C1-2}.

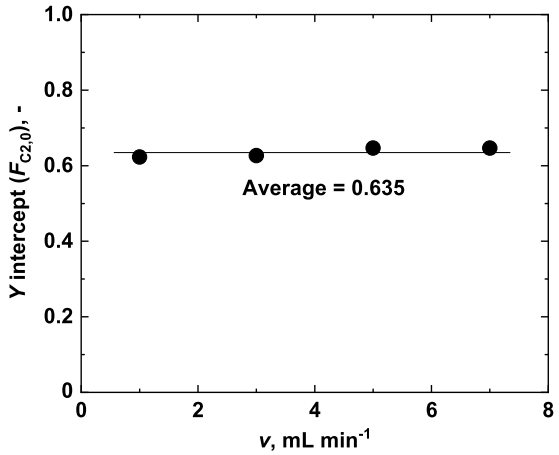

Figure 5. Y-intercepts of the linear relationship between F_{C1-2} vs t for different v's and fixed m_0 at 2.0 g.

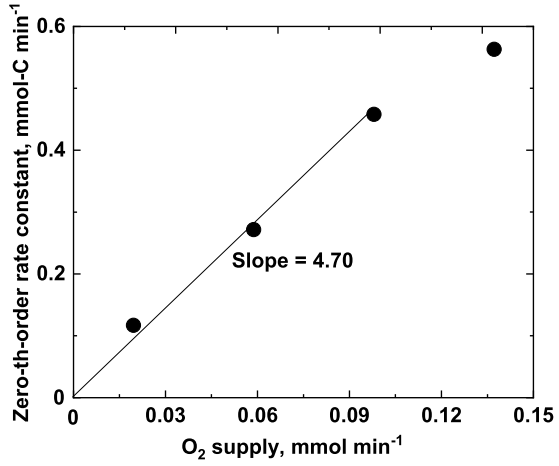

Figure 6. Relationship between the rate of extraction of C2 and that of O_2 supply for m_0 = 2.0 g and v = 1.0, 3.0, 5.0, or 7.0 mL min^{-1}. The rate of C2 extraction was determined by the linear relationship between F_{C2} and t. The O_2 supply was calculated by v and O_2 concentration (19.6 mmol O_2 L^{-1}).

of lignin and hemicellulose from a grass biomass using 0.5−2.0% NaOH without oxidation. Figure 7 shows the changes in F_{C1} with t. For v = 3.0 mL min^{-1}, F_{C1} is described well by

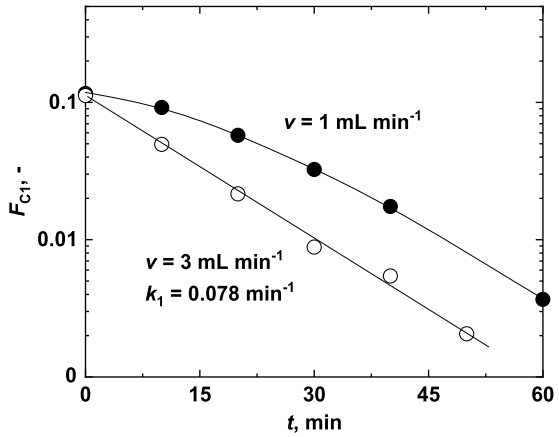

Figure 7. Changes with t of the fraction of C1 for m_0 = 2.0 g. F_{C1} = F_{C1-2} − F_{C2} = 1 − 0.26 exp(−0.000162t) − F_{C2}. F_{C2} was calculated by F_{C2} = −0.00139t + 0.623 for m_0 = 2.0 g and v = 1.0 mL min^{-1} and F_{C2} = −0.00321t + 0.626 for m_0 = 2.0 g and v = 3.0 mL min^{-1}.

assuming first-order kinetics with an apparent rate constant (k_1) of 0.078 min^{-1}. This is consistent with that the pH of the effluent was roughly steady (see Figure S2). On the other hand, for v = 1.0 mL min^{-1}, the apparent rate constant (*i.e.*, the slope of the line) increased with t. This was explained by significant change in pH for t = 0−60 min. The chemical reactions as suggested above consumed hydroxide ions extensively lowering the pH of the aqueous solution particularly in the early period. The kinetic analysis of F_{C1} was not easy for $v \geq$ 5.0 mL min^{-1} due to so fast reaction that completed the extraction of C1 within 10 min, but finally, numerical simulation gave a reasonable value of the rate constant (k_1) of 0.36−0.39 min^{-1}. Thus, to determine k_1, it was necessary to maintain the pH that influenced the rate of C1 extraction significantly.

2.3. Summary of Kinetic Analysis. The kinetics of the primary extraction is described by the following rate equations and eq 2 for the first-order kinetics of the extraction of C3, under the conditions of temperature, 140 °C; O_2 concentration, 19.6 mmol O_2 L^{-1}; and NaOH concentration, 0.1 mol L^{-1}.

$$dX/dt = k_1F_{C1} + k_2F_{C2} + k_3F_{C3} \quad (6)$$

https://dx.doi.org/10.1021/acsomega.0c05154
ACS Omega 2021, 6, 4236−4246

Table 2. Chemical Composition of Solid Left after Oxidative Extraction with m_0 = 2.0 g[a]

			carbohydrates				
experiment	t, min	lignin	glucan	xylan	galactan	mannan	arabinan
cedar		49.8	36.5	4.9	1.6	6.3	0.9
3 mL min^{-1}	160	26.9	65.5	3.4	0.5	3.3	0.6
5 mL min^{-1}	140	6.6	88.9	2.5	0.5	0.7	0.7
7 mL min^{-1}	90	14.3	80.1	3.4	0.6	1.0	0.6

[a]The fractions of the chemical components have been normalized on the carbon bases of the individual solid.

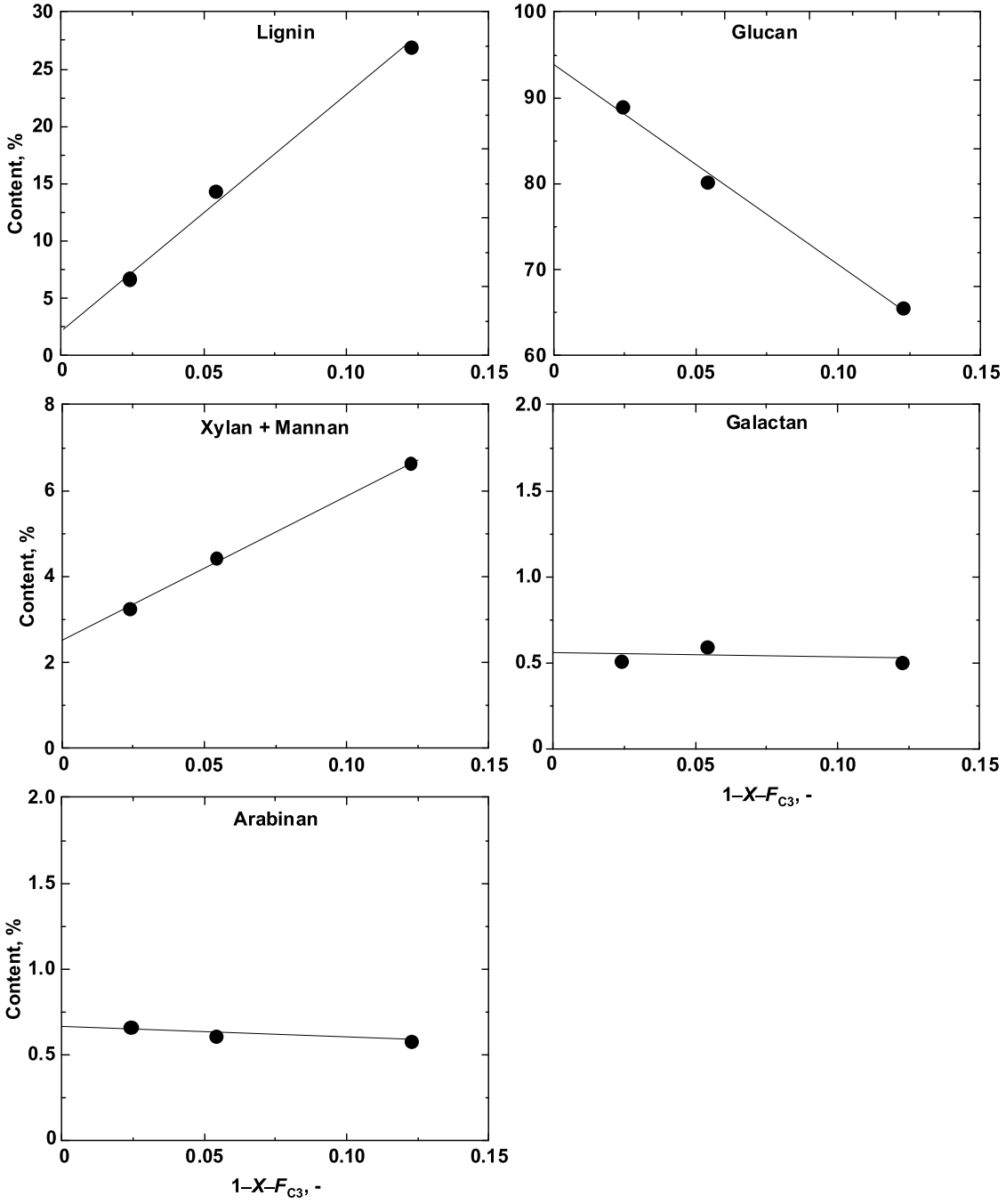

Figure 8. Contents of chemical components in solid as a function of $1 - X - F_{C3}$ ($=F_{C1} + F_{C2}$).

$$F_{C1} = F_{C1,0} \exp(-k_1 t) \approx 0.10 \exp(-0.36t) \quad (7)$$

$$F_{C2} = F_{C2,0} \exp(-k_2 t) \approx 0.64 \exp(-0.034t) \quad (8)$$

k_1 = 0.36 was obtained by the kinetic analysis of the data for m_0 = 2.0 g and v = 5.0 mL min^{-1}. k_2 is a linear function of O_2 concentration. Equation 6 shows that the three components (C1−C3) underwent extraction obeying the first-order kinetics

https://dx.doi.org/10.1021/acsomega.0c05154
ACS Omega 2021, 6, 4236−4246

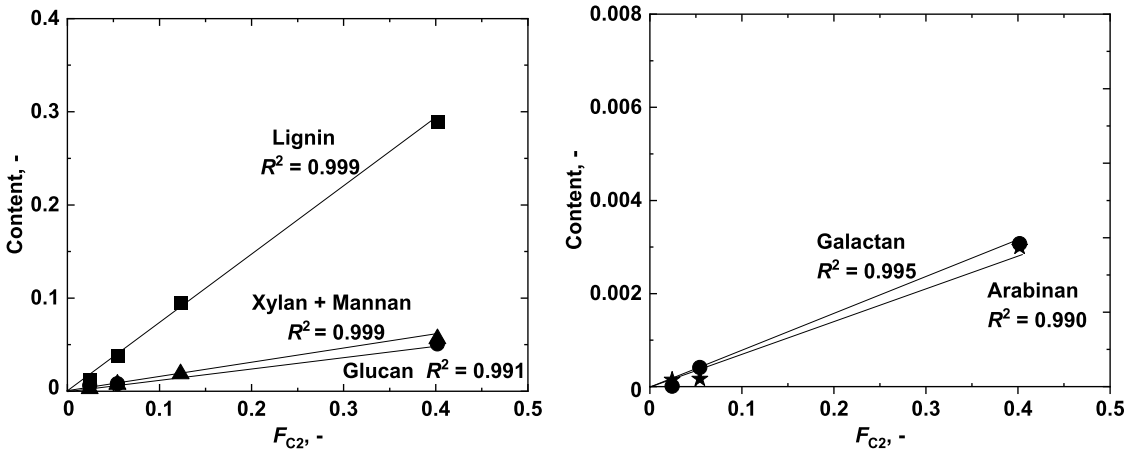

Figure 9. Content of chemical component on the basis of cedar carbon as a function of F_{C2}.

Table 3. Chemical Compositions of C1−C3[a]

kinetic component	lignin	glucan	xylan + mannan	galactan	arabinan	total
C1	0.032 (30.6)	0.036 (34.3)	0.022 (20.9)	0.011 (10.9)	0.003 (3.3)	0.104 (100)
C2	0.360 (56.7)	0.157 (24.7)	0.106 (16.7)	0.006 (1.0)	0.006 (0.9)	0.635 (100)
C3	0.006 (2.4)	0.245 (93.9)	0.006 (2.5)	0.001 (0.6)	0.002 (0.7)	0.261 (100)

[a]The fraction is based on the total carbon involved in cedar. The numbers in parentheses (%) are the carbon-based fractions in C1, C2, or C3.

with respect to their individual fractions. As discussed later, neither C1 nor C2 corresponded simply to a particular chemical component (*e.g.*, the amorphous part of cellulose, lignin, or hemicellulose). In other words, those were mixtures of two or even more chemical components. Nonetheless, in the kinetic sense, all of the components behaved as single reactants. The lignin in cedar is composed of only G units (99.5%),[28] and such a single type of aromatic unit makes the structure of lignin relatively simple. This could be an important reason for the invariance of degradation modes.

2.4. Chemical Composition of C3. The chemical composition of the solid is one of the most important characteristics of the oxidative extraction. Table 2 shows the compositions of the solids after extraction with m_0 = 2.0 g and v = 3.0, 5.0, or 7.0 mL min^{-1}. The data shown in this table allowed us to estimate the chemical composition of C3 as the most refractory component. Figure 8 displays the contents of the individual chemical components in the solid as a function of $1 - X - F_{C3}$ ($= F_{C1} + F_{C2}$). It is noted that every content is a linear function of $1 - X - F_{C3}$. This means that extrapolating the straight line to $1 - X - F_{C3} = 0$ gives the content of the chemical component in C3 as the Y-intercept, assuming that its chemical composition was steady over the range of conversion. The contents of glucan, xylan + mannan, galactan, arabinan, and lignin were 93.9, 2.5, 0.55, 0.66, and 2.41%, respectively. It was thus possible to prepare a pulp with a residual lignin content as small as 2.4% on the carbon basis. However, the complete extraction of C1 and C2 resulted in the yield of solid (as C3) with a cellulose recovery as low as $F_{C3,0}$/(glucan content in the cedar) ≈ 65%.

2.5. Chemical Compositions of C1 and C2. The quantitative knowledge of the chemical composition of C3 allowed us to determine that of C2. The solids after the extraction under the conditions of m_0 = 2.0 g, v = 1.0−7.0 mL min^{-1}, and sufficiently long t consisted of C3 and C2, but no C1. Figure 9 shows the contents of the chemical components as functions of F_{C2}. Each content was calculated straightforwardly as the difference in that between the solid and C3 (of the solid). The content of every chemical component of C2 is a linear function of F_{C2}. This demonstrates that the chemical composition of F_{C2} was steady during the oxidative extraction and also agrees with the behavior of C3 as a single reactant. The initial contents (at t = 0) determined were as follows: lignin, 0.36 on the cedar carbon basis (56.7% of C2); glucan, 0.16 (24.7%); xylan + mannan, 0.11 (16.7%); galactan, 0.006 (1.0%); and arabinan, 0.006 (0.9%).

The initial chemical composition of C1 was determined from those of the cedar, C2, and C3. Table 3 shows the compositions of C1 together with those of C2 and C3. C1 consisted mainly of lignin, glucan, xylan/mannan, and galactan. More importantly, the carbohydrates accounted for 2/3 of C1 on the carbon basis. Thus, hot-compressed alkaline water extracted more carbohydrates than lignin in the absence of O_2. The total fraction of the carbohydrates in C2 was lower than that in C1, but still more than 40%. On the other hand, the major portion of lignin, 90%, was involved in C2, indicating that the oxidation was mandatory for extracting the lignin extensively.

2.6. Selectivities to Products from C2. The products from the extraction were lumped into CO_2, lower organic acid (LOA), acid-soluble lignin (AS-L), acid-insoluble lignin (AI-L), and ethanol-insoluble matter (EI). Among these, AI-L and AS-L were characterized by size-exclusion chromatography (SEC). The molecular mass of AS-L ranged 100−2000 Da (calibrated with polystyrene standards) and clearly differed from that of AI-L over a range up to 100 000 (see Figure S3). AS-L consisted of monomers, dimers, and small amounts of oligomers.[29] LOA was represented by formic, acetic, lactic, glycolic, and oxalic acids (Figure S1), the major portions of which were derived from the carbohydrates and lignin (interaromatic linkages and aromatic rings).[30−33]

The yields of CO_2, LOA, AS-L, AI-L, and EI were analyzed within the ranges of t after complete conversion of C1. Such ranges of t were ≥60, ≥50, ≥30, and ≥20 min for the

https://dx.doi.org/10.1021/acsomega.0c05154
ACS Omega 2021, 6, 4236−4246

conditions of v = 1.0, 3.0, 5.0, and 7.0 mL min^{-1}, respectively, with a fixed m_0 of 2.0 g. In other words, $(1 - X - F_{C3}) = F_{C1} + F_{C2} \approx F_{C2}$. Figure 10 plots the yields of CO_2, LOA, AS-L, AI-L,

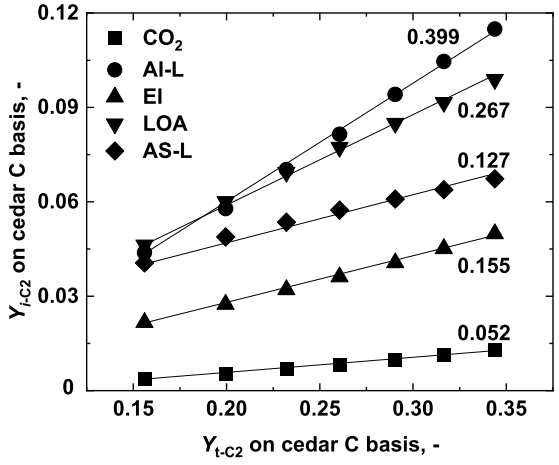

Figure 10. Yields of CO_2, LOA, AI-L, AS-L, and EI from C2 as functions of $F_{C2,0} - F_{C2}$ for m_0 = 2.0 g and v = 1.0 mL min^{-1}. The numbers indicated in the frame are slopes of the corresponding straight lines, *i.e.*, selectivities to the products.

and EI against Y_{C2}, which is defined by $Y_{C2} = F_{C2,0} - F_{C2} \approx 0.635 - F_{C2}$. All of the yields increase linearly with Y_{C2} but with different slopes, which correspond directly to the selectivities to the corresponding products from C2. This trend reveals no or very little change in the product selectivity and agrees well with the steady chemical composition of C2, strongly supporting the behavior of C2 as a single reactant. It is known that O_2-derived active species can directly attack electron-rich aromatic and olefinic moieties and also aliphatic chains connected to aromatic ring systems.[34,35] It is therefore hypothesized that such active species indiscriminately attacked the lignin as well as associated carbohydrates (hemicellulose and cellulose), and this resulted in simultaneous and synchronized extraction from the different chemical components of C2. This hypothesis is supported by Yokoyama et al.[36] who found that the O_2 active species generated by a phenolic compound (2,4,6-trimethylphenol) attacked a carbohydrate (a model compound; methyl *p*-D-glucopyranoside) in an alkaline environment.

The product selectivities were also determined for v = 3.0, 5.0, and 7.0 mL min^{-1}. The result is shown in Figure 11. The selectivities are almost steady at $v \geq$ 3.0 mL min^{-1}, while those to AS-L and EI decreases and increases at v = 1.0−3.0 mL min^{-1}, respectively. In addition, the selectivity to LOA slightly decreases at v = 1.0−3.0 mL min^{-1}. Such influences of v on the selectivities to AS-L, EI, and LOA can be explained by chemical bonding between fragments of lignin and carbohydrates. EI at $v \geq$ 3.0 mL min^{-1} carried lignin fragments (as AS-L precursor), but it was partly decomposed to EI, AS-L, and LOA by decreasing v below 3.0 mL min^{-1} (*i.e.*, by extending the residence time of the primary product). Such an aqueous-phase secondary reaction decreased the selectivity to EI while increasing those to AS-L and LOA. In fact, the decrease in the selectivity to EI seems to be compensated by the increases in those to AS-L and LOA at v = 3.0−1.0 mL min^{-1}. The O_2 consumption was complete under the conditions of m_0 = 2.0 g, regardless of v. Aqueous-phase base-catalyzed hydrolysis of carbohydrates,[37,38] which did not require O_2, would be an

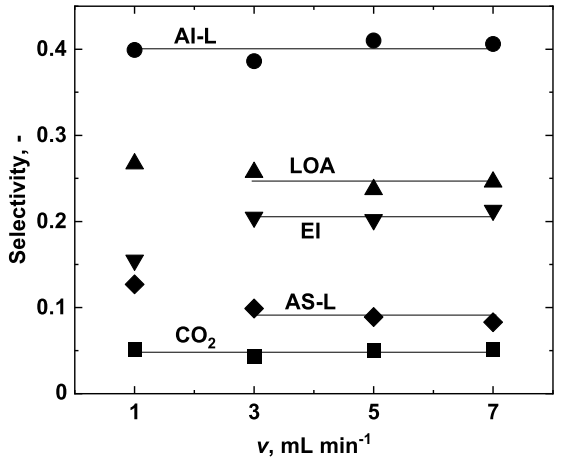

Figure 11. Effects of v on selectivities to AI-L, AS-L, LOA, EI, and CO_2 for conversion of C_2. m_0: 2.0 g.

important secondary reaction to change the product distribution.

Figure 12 contrasts the chemical composition of C2 and primary product distribution. The sum of the AI-L and AS-L

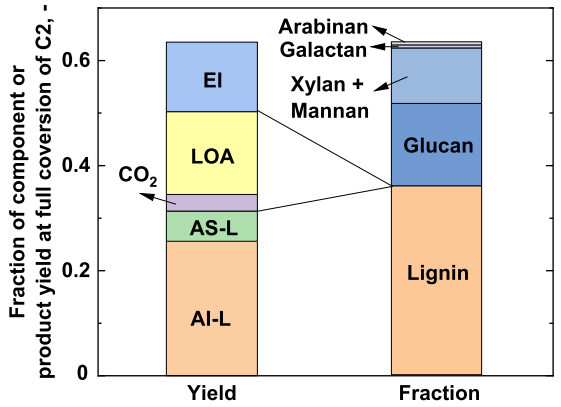

Figure 12. Contrast between the chemical composition of C2 and product yields from C2.

yields, 0.314, is smaller than, but close to, the lignin content in C2. Considering that EI contains lignin fragments to be released by the secondary reaction, the total yields of AI-L and AS-L are even closer to the lignin content. Their yields for m_0 = 2.0 g and v = 1.0 mL min^{-1} were an example. The relationship between AI-L plus AS-L yields and lignin content thus shows that the lignin was converted mainly into AI-L and AS-L but minimally into LOA and CO_2, even though the degradation of C2 was caused by the oxidation. LOA and CO_2 were rather formed from the degradation of the carbohydrates. It is then hypothesized that the oxidative extraction was caused by the oxidation of the lignin−carbohydrate complex (LCC) and the resultant release of lignin fragments together with LOA and CO_2 mainly from the carbohydrate part.[39] It was also estimated that LCC of EI was carbohydrate-rich and therefore insoluble in ethanol.

2.7. Selectivities to Products from C1. Quantitative knowledge of the product selectivities for the C2 conversion allowed us to derive those for C1. F_{C2} is expressed as a function of t.

$$F_{C2} = F_{C2,0} - k_2 t \quad (9)$$

https://dx.doi.org/10.1021/acsomega.0c05154
ACS Omega 2021, 6, 4236−4246

As shown in Figure 10, the individual products from C2 are expressed as follows

$$Y_{i-C2} = (F_{C2,0} - F_{C2})S_{i-C2} = Y_{t-C2}S_{i-C2} \quad (10)$$

where $Y_{i\text{-}C2}$, $Y_{t\text{-}C2}$, and $S_{i\text{-}C2}$ are the yield of product i, the total product yield from C2, and selectivity to i from C2, respectively. The yield of product i from C1 is then given by

$$Y_{i-C1} = Y_i - Y_{i-C2} = Y_{t-C1}S_{i-C1} \quad (11)$$

where $Y_{i\text{-}C1}$ and Y_i are the yield of i from C1 and the total yield of i (from C1 and C2), respectively. Strictly saying, it is necessary to consider the products from not only C2 but also C3. But the latter can be ignored due to extremely slow degradation of C3.

Figure 13 shows the calculated $Y_{i\text{-}C1}$ as a function of $Y_{t\text{-}C1}$. Every $Y_{i\text{-}C1}$ increases linearly with $Y_{t\text{-}C1}$. It is thus reasonable to

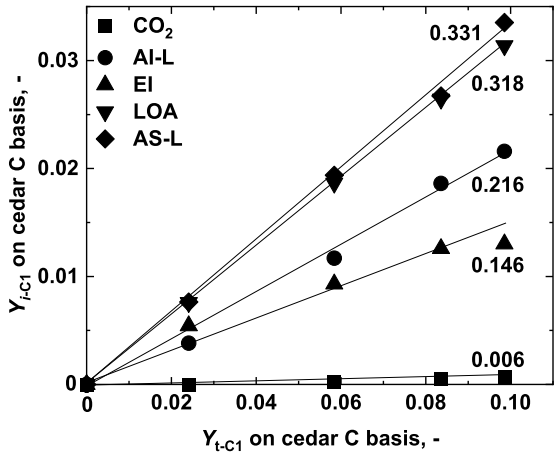

Figure 13. Yields of CO_2, LOA, AI-L, AS-L, and EI from C1 as functions of $F_{C1,0} - F_{C1}$ for m_0 = 2.0 g and v = 1.0 mL min^{-1}. The numbers indicated in the graphs are slopes of the straight lines, *i.e.*, selectivities to the individual products.

Table 4. Selectivities to Products from C1

v, mL min^{-1}	CO_2	LOA	AS-L	AI-L	EI
1.0	0.0060	0.32	0.33	0.22	0.15
3.0	0.0077	0.31	0.30	0.25	0.16
5.0	0.0053	0.33	0.32	0.20	0.18
average $S_{i\text{-}C1}$	0.0063	0.32	0.32	0.22	0.16

determine the selectivity, $S_{i\text{-}C1}$. Table 4 lists the selectivities for different v's, showing no or little influence of v on the selectivities, *i.e.*, no or little progress of the aqueous-phase secondary reaction of the primary extract from C1. The selectivity to CO_2 was below 0.01, and this was consistent with that C1 underwent nonoxidative degradation (or just dissolution). Figure 14 compares the product yields from C1 with its chemical composition. It is believed that LOA as well as EI was derived from the carbohydrates, according to previous studies, which showed hydrolytic degradation of hemicellulose- and cellulose-produced oligosaccharides and LOA.[40,41] More importantly, the sum of AS-L and AI-L yields is clearly greater than the lignin content of C1. This can be explained only by that AS-L and/or AI-L chemically incorporated carbohydrates forming LCC. It was also believed

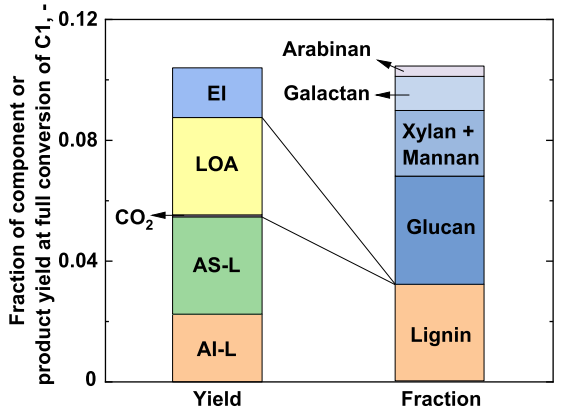

Figure 14. Contrast between the chemical composition of C1 and product yields from C1.

that the LCC was lignin-rich, and then recovered as a portion of AS-L, or otherwise, AI-L. Baptista et al.[17] reported that the pine lignin obtained by the conventional kraft cook (NaOH and Na_2S) at 170 °C contains about 4 wt % carbohydrates, and shortening the residence time can increase the carbohydrate content. More detailed chemical analysis of AS-L and AI-L is necessary for clarifying the abundance and chemical structure of LCC and deeper understanding of the mechanism of C1 degradation in the future work. On the other hand, for the C2 degradation, more analysis of EI is needed for characterization of LCC that would be abundant in carbohydrate-rich LCC.

3. CONCLUSIONS

The oxidative extraction of the cedar in the flow-through percolator and the combined analysis of the kinetics of extraction and chemical compositions of the products have demonstrated the following within the ranges of experimental conditions:

(1) A sufficiently small mass of the cedar and large liquid flow rate (*i.e.*, O_2 feeding rate) allowed us to determine the rate of the primary extraction, eliminating the rate-limiting physical processes. The primary extract can be recovered by eliminating its secondary reactions in the aqueous phase and over the surface of solid being extracted.

(2) Limiting the rate of O_2 supply allows us to derive three kinetic components, C1−C3, quantitatively.

(3) All of C1, C2, and C3 undergo degradation following first-order kinetics with respect to their carbon-based fractions, F_{C1}, F_{C2}, and F_{C3}, respectively. C1 is converted by nonoxidative reactions such as ion exchange and base-catalyzed hydrolysis, while C2 and C3 are converted by oxidation. C3 is much more refractory than C2 as well as C1.

(4) The chemical analysis of solids at different conversions allows us to clarify the chemical compositions of the individual kinetic components.

(5) The individual kinetic components are chemical mixtures of lignin and carbohydrates, but they behave as single reactants while maintaining their chemical compositions. The product selectivities are therefore steady over the ranges of their conversions. LCC is abundant in C1 and C2, playing important roles in the product selectivities.

https://dx.doi.org/10.1021/acsomega.0c05154
ACS Omega 2021, 6, 4236−4246

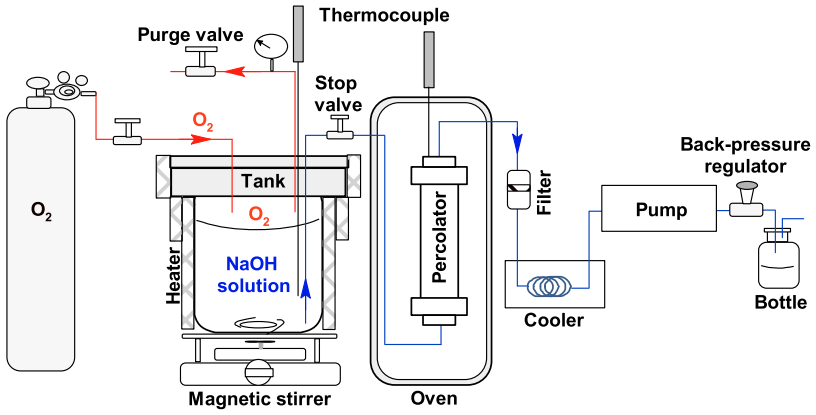

Figure 15. Setup of the experimental system.

(6) C3 as the refractory component consists of glucan and other carbohydrates with the total content as high as 98% on the carbon basis, but C3 accounts for only 26% of the cedar.

4. EXPERIMENTAL SECTION

4.1. Materials. Woodchips of a type of Japanese cedar (*Cryptomeria japonica*) trunk, produced in Oita prefecture, Japan, were pulverized to sizes smaller than 0.85 mm, vacuum-dried at 60 °C for 12 h, and used as the feedstock. The particle sizes of the feedstock were well below a critical size of woodchips (thickness ≈ 4 mm) for eliminating the intrasolid diffusional effects on the kinetics of extraction.[42] The chemical composition of the cedar was as follows: carbohydrates, 50.2 (glucan, 36.5; xylan, 4.9; galactan, 1.6; mannan, 6.3; arabinan, 0.9); lignin, 49.8, on the carbon basis of the cedar free from ash, acetyl, extractives, and ash with contents of 1.4, 0.7, and 0.9 wt % on a dry basis, respectively. The following compounds were purchased from FUJIFILM Wako Pure Chemical Co. or Tokyo Chemical Industry Co. Ltd.: glucose, xylose, arabinose, galactose, mannose, acetic acid, formic acid, oxalic acid, lactic acid, glycolic acid, ethanol, sodium hydroxide (NaOH), hydrochloric acid (HCl), and sulfuric acid (H_2SO_4).

4.2. Oxidation in Percolator. Figure 15 shows the experimental setup for the oxidative extraction. The tubular percolator (material; SUS316 tubes and Swagelok connectors, volume; 20.5 mL) was charged with a prescribed mass (0.1−2.0 g) of the cedar, filled with O_2-free 0.1 mol L^{-1} NaOH aq, and connected to the tank storing 0.1 mol L^{-1} NaOH aq (upstream side) and filter (downstream). The tank (volume, 1 L) was heated at 140 °C and pressurized with 2.0 MPa O_2 until saturation. The O_2 concentration in the NaOH aq was measured and determined as 19.6 mmol O_2 L^{-1}, which was roughly in agreement with that calculated according to a previous report, 18.1 mmol O_2 L^{-1}.[43] The oxidative extraction was preliminarily investigated at different temperatures, and it was found that the lignin extraction was very slow at temperatures below 140 °C. It was then chosen for operating the oxidative extraction, while minimization of the secondary reaction was considered.

The percolator was heated to 140 °C, and the temperature was held for 20 min without supply of O_2. Then, the O_2-saturated NaOH aq was fed to the percolator at a steady flow rate in the range of 1.0−7.0 mL min^{-1}. The start time of the oxidative extraction was defined as the time at which the liquid flow occurred by the pump. The effluent liquid was collected in glass bottles at the downstream of the pump with fixed intervals of 10 min. The temperature and pressure inside the percolator were maintained exactly the same as those of the tank to avoid release of O_2 out of the NaOH aq. The liquid residence time within the cedar fixed bed (2.5 mm thickness in the case of 0.10 g of initial mass) was 2.5 s when a flow rate of 5.0 mL min^{-1} was applied. After the run for the prescribed time, the percolator was cooled down to room temperature. The solid was taken out of the percolator, washed exhaustively with pure water (electrical resistance, 18.2 MΩ), and then dried under vacuum at 60 °C for 12 h prior to weighing and analyses.

4.3. Product Separation and Analyses. Figure 16 shows the flowchart of product separation and analyses. Immediately after the run, the total organic carbon (TOC) and inorganic carbon (IC) dissolved in the recovered liquid were quantified

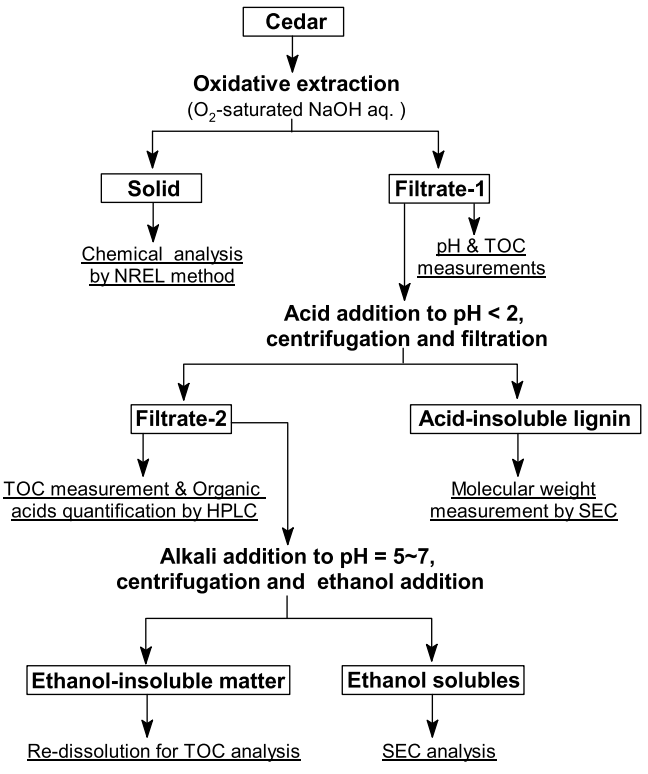

Figure 16. Scheme of product separation, collection, and analyses. SEC, size-exclusion chromatography.

https://dx.doi.org/10.1021/acsomega.0c05154
ACS Omega 2021, 6, 4236−4246

with a Shimadzu TOC-5000A analyzer (Shimadzu Corp., Kyoto, Japan). The product gas that consisted solely of CO_2 was quantified as IC. A portion of every recovered liquid was acidified to pH < 2 by adding HCl aq for precipitating and recovering the AI-L. The acidified liquid after separated from AI-L was subjected to TOC measurement and quantification of LOA with a high-performance liquid chromatography (HPLC) system (Shimadzu, LC-20 Prominence series, Shimadzu Corp., Kyoto, Japan) and a type of column (Bio-Rad Aminex HPX-87H column 300 × 7.8 mm^2). The acidified liquid was neutralized by adding NaOH aq, concentrated by rotary evaporation, and then adding ethanol. This process caused precipitation of solid consisting mainly of oligosaccharides, allowing the organic acid and AS-L to remain dissolved in the acidic ethanol/water. The chemical composition of the solid residue was determined by a standard analytical procedure of NREL *via* two-stage hydrolysis.[44] The carbon-based content of each chemical component (glucan, xylan, mannan, galactan, arabinan, and lignin) in the residue was then determined according to their monomers formula: glucan, $[C_6H_{10}O_5]_n$ (carbon content of the monomer is 72/162); galactan, $[C_6H_{10}O_5]_n$ (72/162); mannan, $[C_6H_{10}O_5]_n$ (72/162); xylan, $[C_5H_8O_4]_n$ (60/132); and arabinan, $[C_5H_8O_4]_n$ (60/132). In addition, the lignin in the cedar consisted solely of guaiacyl units $[C_{10}H_{12}O_5]_n$ (120/212).[28]

The above-mentioned method gave the distribution of carbon over the range from the solid residue to CO_2 quantitatively. The yields of the solid residue, AI-L, ethanol-insoluble matter (EI), AS-L, LOA, and CO_2 are denoted by $Y_{AI\text{-}L}$, Y_{EI}, $Y_{AS\text{-}L}$, Y_{LOA}, and Y_{CO_2}, respectively. These yields were defined by

$$Y_i = m_i/m_{t,0}$$

where m_i is the carbon-based amount of i and $m_{t,0}$ is the total amount of carbon involved in the solid at time $(t) = 0$. The overall carbon-based conversion to extract was defined by

$$X = 1 - m_t/m_{t,0} = Y_{AI-L} + Y_{AS-L} + Y_{EI} + Y_{LOA} + Y_{CO_2}$$

4.4. Quantitative Kinetic Analysis. The three kinetic components in the cedar were represented by C1−C3. C1-2 represents the sum of C1 and C2. X is the overall carbon-based conversion. $F_{C1\text{-}2}$ was defined as the carbon-based fraction of C1-2. F_{C1}, F_{C2}, and F_{C3} were defined as the carbon-based fractions of C1, C2, and C3, respectively.

■ ASSOCIATED CONTENT

Supporting Information

The Supporting Information is available free of charge at https://pubs.acs.org/doi/10.1021/acsomega.0c05154.

Cedar-carbon-based product distribution and lower organic acid yields for m_0 = 2.0 g, v = 5.0 mL min^{-1} (Figure S1); changes in pH of effluent liquid at percolator exit for m_0 = 2.0 g (Figure S2); SEC chromatograms for AI-L and AS-L (Figure S3); and selectivity to product from C2 for the different conditions (Table S1) (PDF)

■ AUTHOR INFORMATION

Corresponding Author

Jun-ichiro Hayashi − *Interdisciplinary Graduate School of Engineering Sciences, Institute for Materials Chemistry and Engineering, and Transdisciplinary Research and Education Center of Green Technology, Kyushu University, Kasuga, Fukuoka 816-8580, Japan;* orcid.org/0000-0001-5068-4015; Email: junichiro_hayashi@cm.kyushu-u.ac; Fax: +81 092-583-7793

Authors

Jing-Xian Wang − *Interdisciplinary Graduate School of Engineering Sciences, Kyushu University, Kasuga, Fukuoka 816-8580, Japan;* orcid.org/0000-0002-8145-1350

Shusaku Asano − *Interdisciplinary Graduate School of Engineering Sciences and Institute for Materials Chemistry and Engineering, Kyushu University, Kasuga, Fukuoka 816-8580, Japan;* orcid.org/0000-0001-6297-057X

Shinji Kudo − *Interdisciplinary Graduate School of Engineering Sciences, Institute for Materials Chemistry and Engineering, and Transdisciplinary Research and Education Center of Green Technology, Kyushu University, Kasuga, Fukuoka 816-8580, Japan;* orcid.org/0000-0003-0002-796X

Complete contact information is available at: https://pubs.acs.org/10.1021/acsomega.0c05154

Notes

The authors declare no competing financial interest.

■ ACKNOWLEDGMENTS

This work was supported by Council for Science, Technology and Innovation (CSTI), Cross-ministerial Strategic Innovation Promotion Program (SIP), "Technologies for Smart Bio-industry and Agriculture" administered by Bio-oriented Technology Research Advancement Institution, and National Agriculture and Food Research Organization. The authors are also grateful to the Cooperative Research Program of Network Joint Research Center for Materials and Devices that has been supported by Ministry of Education, Culture, Sports, Science, and Technology, Japan. Jingxian Wang acknowledges the China Scholarship Council (grant number: 201706420069) for his financial support.

■ REFERENCES

(1) Mosier, N.; Wyman, C.; Dale, B.; Elander, R.; Lee, Y. Y.; Holtzapple, M.; Ladisch, M. Features of promising technologies for pretreatment of lignocellulosic biomass. *Bioresour. Technol.* **2005**, *96*, 673−686.

(2) Hendriks, A. T. W. M.; Zeeman, G. Pretreatments to enhance the digestibility of lignocellulosic biomass. *Bioresour. Technol.* **2009**, *100*, 10−18.

(3) Kawamata, Y.; Yoshikawa, T.; Aoki, H.; Koyama, Y.; Nakasaka, Y.; Yoshida, M.; Masuda, T. Kinetic analysis of delignification of cedar wood during organosolv treatment with a two-phase solvent using the unreacted-core model. *Chem. Eng. J.* **2019**, *368*, 71−78.

(4) Lee, R. L. The grand challenge of cellulosic biofuels. *Nat. Biotechnol.* **2017**, *35*, 912−915.

(5) Posoknistakul, P.; Akiyama, T.; Yokoyama, T.; Matsumoto, Y. Stereo-preference in the degradation of the erythro and threo isomers of β-O-4-type lignin model compounds in oxidation processes: Part 1: In the reaction with active oxygen species under oxygen delignification conditions. *J. Wood Chem. Technol.* **2016**, *36*, 288−303.

(6) Mittal, A.; Katahira, R.; Donohoe, B. S.; Black, B. A.; Pattathil, S.; Stringer, J. M.; Beckham, G. T. Alkaline peroxide delignification of corn stover. *ACS Sustainable Chem. Eng.* **2017**, *5*, 6310−6321.

(7) Arvaniti, E.; Bjerre, A. B.; Schmidt, J. E. Wet oxidation pretreatment of rape straw for ethanol production. *Biomass Bioenergy* **2012**, *39*, 94−105.

(8) Martín, C.; Klinke, H. B.; Thomsen, A. B. Wet oxidation as a pretreatment method for enhancing the enzymatic convertibility of sugarcane bagasse. *Enzyme Microb. Technol.* **2007**, *40*, 426−432.
(9) Kim, J. S.; Lee, Y. Y.; Kim, T. H. A review on alkaline pretreatment technology for bioconversion of lignocellulosic biomass. *Bioresour. Technol.* **2016**, *199*, 42−48.
(10) Morone, A.; Sharma, G.; Sharma, A.; Chakrabarti, T.; Pandey, R. A. Evaluation, applicability and optimization of advanced oxidation process for pretreatment of rice straw and its effect on cellulose digestibility. *Renewable Energy* **2018**, *120*, 88−97.
(11) Kim, S.; Holtzapple, M. T. Delignification kinetics of corn stover in lime pretreatment. *Bioresour. Technol.* **2006**, *97*, 778−785.
(12) Chiang, V. L.; Yu, J.; Eckert, R. C. Isothermal reaction kinetics of kraft delignification of douglas-fir. *J. Wood Chem. Technol.* **1990**, *10*, 293−310.
(13) Lourenço, A.; Gominho, J.; Marques, A. V.; Pereira, H. Reactivity of syringyl and guaiacyl lignin units and delignification kinetics in the kraft pulping of Eucalyptus globulus wood using Py-GC-MS/FID. *Bioresour. Technol.* **2012**, *123*, 296−302.
(14) Jafari, V.; Nieminen, K.; Sixta, H.; Heiningen, A. V. Delignification and cellulose degradation kinetics models for high lignin content softwood Kraft pulp during flow-through oxygen delignification. *Cellulose* **2015**, *22*, 2055−2066.
(15) Klinke, H. B.; Ahring, B. K.; Schmidt, A. S.; Thomsen, A. B. Characterization of degradation products from alkaline wet oxidation of wheat straw. *Bioresour. Technol.* **2002**, *82*, 15−26.
(16) Ding, N.; Song, X. Q.; Jiang, Y. T.; Luo, B.; Zeng, X. H.; Sun, Y.; Tang, X.; Lei, T. Z.; Lin, L. Cooking with active oxygen and solid alkali facilitates lignin degradation in bamboo pretreatment. *Sustainable Energ. Fuels* **2018**, *2*, 2206−2214.
(17) Baptista, C.; Robert, D.; Duarte, A. P. Effect of pulping conditions on lignin structure from maritime pine kraft pulps. *Chem. Eng. J.* **2006**, *121*, 153−158.
(18) Shi, J. B.; Yang, Q. L.; Lin, L. Structural features and thermal characterization of bagasse hemicelluloses obtained from the yellow liquor of active oxygen cooking process. *Polym. Degrad. Stab.* **2013**, *98*, 550−556.
(19) de Carvalho Oliveira, F.; Srinivas, K.; Helms, G. L.; Isern, N. G.; Cort, J. R.; Goncalves, A. R.; Ahring, B. K. Characterization of coffee (*Coffea arabica*) husk lignin and degradation products obtained after oxygen and alkali addition. *Bioresour. Technol.* **2018**, *257*, 172−180.
(20) Jafari, V.; Sixta, H.; Heiningen, A. V. Kinetics of oxygen delignification of high-kappa pulp in a continuous flow-through reactor. *Ind. Eng. Chem. Res.* **2014**, *53*, 8385−8394.
(21) Yang, R.; Lucia, L.; Ragauskas, A. J.; Jameel, H. Oxygen delignification chemistry and its impact on pulp fibers. *J. Wood Chem. Technol.* **2003**, *23*, 13−29.
(22) Kashimura, N.; Hayashi, J.; Chiba, T. Degradation of a Victorian brown coal in sub-critical water. *Fuel* **2004**, *83*, 353−358.
(23) Yu, Y.; Wu, H. W. Characteristics and precipitation of glucose oligomers in the fresh liquid products obtained from the hydrolysis of cellulose in hot-compressed water. *Ind. Eng. Chem. Res.* **2009**, *48*, 10682−10690.
(24) Ji, Y.; Wheeler, M. C.; Heiningen, A. V. Oxygen delignification kinetics: CSTR and batch reactor comparison. *AIChE J.* **2007**, *53*, 2681−2687.
(25) Sierra-Ramírez, R.; Garcia, L. A.; Holtzapple, M. T. Selectivity and delignification kinetics for oxidative short-term lime pretreatment of poplar wood, Part I: Constant-pressure. *Biotechnol. Prog.* **2011**, *27*, 976−985.
(26) Fu, S. Y.; Lucia, L. A. Investigation of the chemical basis for inefficient lignin removal in softwood kraft pulp during oxygen delignification. *Ind. Eng. Chem. Res.* **2003**, *42*, 4269−4276.
(27) Kataria, R.; Ruhal, R.; Babu, R.; Ghosh, S. Saccharification of alkali treated biomass of Kans grass contributes higher sugar in contrast to acid treated biomass. *Chem. Eng. J.* **2013**, *230*, 36−47.
(28) Tarmadi, D.; Tobimatsu, Y.; Yamamura, M.; Miyamoto, T.; Miyagawa, Y.; Umezawa, T.; Yoshimura, T. NMR studies on lignocellulose deconstructions in the digestive system of the lower termite *Coptotermes formosanus* Shiraki. *Sci. Rep.* **2018**, *8*, No. 1290.
(29) Katahira, R.; Mittal, A.; McKinney, K.; Chen, X. W.; Tucker, M. P.; Johnson, D. K.; Beckham, G. T. Base-catalyzed depolymerization of biorefinery lignins. *ACS Sustainable Chem. Eng.* **2016**, *4*, 1474−1486.
(30) Zhang, D. C.; Chai, X. S.; Hou, Q. X.; Ragauskas, A. Characterization of fiber carboxylic acid development during one-stage oxygen delignification. *Ind. Eng. Chem. Res.* **2005**, *44*, 9279−9285.
(31) Jafari, V.; Labafzadeh, S. R.; King, A.; Kilpeläinen, I.; Sixta, H.; Heiningen, A. V. Oxygen delignification of conventional and high alkali cooked softwood Kraft pulps, and study of the residual lignin structure. *RSC Adv.* **2014**, *4*, 17469−17477.
(32) Pola, L.; Collado, S.; Oulego, P.; Calvo, P. Á.; Díaz, M. Characterisation of the wet oxidation of black liquor for its integration in Kraft paper mills. *Chem. Eng. J.* **2021**, *405*, No. 126610.
(33) Wang, J. X.; Asano, S.; Kudo, S.; Hayashi, J. I. Deep Delignification of Woody Biomass by Repeated Mild Alkaline Treatments with Pressurized O_2. *ACS Omega* **2020**, *5*, 29168−29176.
(34) Gierer, B. J.; Yang, E.; Reitberger, T. On the significance of the superoxide radical ($O_2\bullet^-$/$HO_2\bullet$) in oxidative delignification, dtudied with 4-*t*-butylsyringol and 4-*t*-butylguaiacol. Part I. The mechanisrn of aromatic ring opening. *Holzforschung* **1994**, *48*, 405−414.
(35) Gierer, J. Formation and involvement of superoxide ($O_2\bullet^-$/$HO_2\bullet$) and hydroxyl (OH•) radicals in TCP bleaching processes: a review. *Holzforschung* **1997**, *51*, 34−46.
(36) Yokoyama, T.; Matsumoto, Y.; Meshitsuka, G. Reaction selectivity of active oxygen species in oxygen-alkali bleaching. *J. Wood Chem. Technol.* **1999**, *19*, 187−202.
(37) Castro, R. C. D. A.; Fonseca, B. G.; Santos, H. T. L. D.; Ferreira, I. S.; Mussatto, S. I.; Roberto, I. C. Alkaline deacetylation as a strategy to improve sugars recovery and ethanol production from rice straw hemicellulose and cellulose. *Ind. Crops Prod.* **2017**, *106*, 65−73.
(38) Farhat, W.; Venditti, R.; Quick, A.; Taha, M.; Mignard, N.; Becquart, F.; Ayoub, A. Hemicellulose extraction and characterization for applications in paper coatings and adhesives. *Ind. Crops Prod.* **2017**, *107*, 370−377.
(39) Lawoko, M.; Henriksson, G.; Gellerstedt, G. Structural differences between the lignin-carbohydrate complexes present in wood and in chemical pulps. *Biomacromolecules* **2005**, *6*, 3467−3473.
(40) Knill, C. J.; Kennedy, J. F. Degradation of cellulose under alkaline conditions. *Carbohydr. Polym.* **2003**, *51*, 281−300.
(41) Jin, F. M.; Zhou, Z. Y.; Moriya, T.; Kishida, H.; Higashijima, H.; Enomoyo, H. Controlling hydrothermal reaction pathways to improve acetic acid production from carbohydrate biomass. *Environ. Sci. Technol.* **2005**, *39*, 1893−1902.
(42) Dang, V. Q.; Nguyen, K. L. A universal kinetic model for characterisation of the effect of chip thickness on kraft pulping. *Bioresour. Technol.* **2008**, *99*, 1486−1490.
(43) Tromans, D. Modeling oxygen solubility in water and electrolyte solutions. *Ind. Eng. Chem. Res.* **2000**, *39*, 805−812.
(44) Sluiter, B. H. A.; Ruiz, R.; Scarlata, C.; Sluiter, J.; Templeton, D.; Crocker, D. Determination of Structural Carbohydrates and Lignin in Biomass. *Laboratory Analytical Procedure*; National Renewable Energy Laboratory: Golden, CO, 2012. https://www.nrel.gov/docs/gen/fy13/42618.pdf.

https://dx.doi.org/10.1021/acsomega.0c05154
ACS Omega 2021, 6, 4236−4246